Assessment of Evapotranspiration Using Remote Sensing Data and Grid Computing and Application

[1]CRISTINA SERBAN, [2]CARMEN MAFTEI & [3]ALINA BARBULESCU
[1,2] Faculty of Civil Engineering
[3]Faculty of Mathematics and Computers Science
Ovidius University of Constanta
124 Mamaia Blvd.
ROMANIA
[1]serban.cristina@univ-ovidius.ro, [2]cmaftei@univ-ovidius.ro
alinadumitriu@yahoo.com http://alina.ilinc.ro/

Abstract: - The estimation of evapotranspiration (ET) plays an essential role in all activities related to water resources management. In this study we developed a procedure to calculate the spatial distribution of evapotranspiration using remote sensing data. What distinguishes it from other procedures is the use of Grid Computing technique to calculate the evapotranspiration at regional scale and to manage the distributed data sets. One other merit is that it requires a small number of inputs, all other data such net radiation, soil heat flux, albedo, etc., were obtained from remote sensing data. This procedure calculates also the NDVI (Normalized Difference Vegetation Index) and LST (Land Surface Temperature) and offer as a result the corresponding thematic maps. A Web-based client interface has been also built in order to provide the application with Internet-based accessibility. The procedure has been applied to the Dobrogea region located in the south-east of Romania, using a Landsat ETM+ image acquired in 7th June 2000. The evapotranspiration was retrieved during satellite overpass and integrated for 24 hours on pixel-by-pixel base for daily estimation. The estimated evapotranspiration has been compared with local measurements. The results obtained are promising and appear to provide acceptable estimation over the study area.

Key-Words: - remote sensing, Grid computing, evapotranspiration, land surface temperature

1 Introduction

Evapotranspiration (ET) represents the water loss by evaporation and plants transpiration [1]. Estimating the distribution of the evapotranspiration is essential for understanding the water cycle of natural systems and for the management of water resources in landscape systems. In most studies concerning hydrological research or design of hydro-technical systems the determination water loss by evapotranspiration represents the most important item of water balance. Unfortunately there are no experimental techniques well established to estimate the spatial distribution of the ET [24], even if the measurement gauges are allowing today an accurate estimation of the punctual ET.

Considerable progress has been made after Thornthwaite (1948) introduced the concept of evapotranspiration. Many methods have been implemented in order to estimate ET for some particular weather conditions. These can be classified as follows [19]:

(i) water balance method, which is based on the mass conservation principle applied to a given control volume (lysimeter, pan-evaporimeter, etc.),

(ii) energy balance methods,

(iii)empirical and semi-empirical methods (Thornthwaite 1938),

(iv) aerodynamics methods,

(v) combined methods, based on the original Penman (1948) method: they combine two terms: the radiation and the aerodynamic terms.

The analysis of performances of those methods emphasizes the necessity to formulate a "standard" evapotranspiration calculation. Therefore FAO Penman-Monteith [1] has been chosen as standard method for estimating ET. With all efforts done, there are still some issues which make difficult the ET's estimation. We mention the following:

(i) ET values are valid only for homogenous area related to the weather station for which the estimations were made and in the weather conditions of that particular area,

(ii) the necessity to have many weather data,

(iii) in order to determine the spatial distribution of ET, the ET values for several stations should be known afterwards, implying the use of miscellaneous methods of interpolation,

(iv) knowledge concerning the vegetation type

and its development stage, as crop coefficient.

Remote sensing has been considered as the most promising tool for spatial evapotranspiration (ET) estimations [27]. Many studies have been conducted to estimate the evapotranspiration on a large scale, using remote sensing data. Courault et al. [6] present a classification of the methods used to estimate the evapotranspiration:

(i) empirical direct method, where the data coming out from satellite images processing are inserted as entry values in the empirical - semi/ empirical ET estimation models. Harmsen E. et al. [7] presents a technique in which satellite solar insolation estimates are used to predict daily reference evapotranspiration (ETo) using the Penman-Monteith (PM), Preistly-Taylor (PT) and Hargreaves-Samini (HS) methods for Puerto Rico. Also, authors of [8] introduce a method for remotely estimating hourly actual evapotranspiration from short natural vegetation or agricultural crops which consists of equating the ET flux equations based on the generalized Penman-Monteith (GPM) combination method and a humidity gradient (HG) method.

(ii) residual methods of the energy budget which combining empirical methods with physical components (SEBAL, S-Sebi),

(iii) indirect methods (ISBA, Meso-NH).

As example, the paper [23] presents the potential of using an artificial neural network (ANN) for reference evapotranspiration (ETo) estimation with minimum climatic data. The ANN algorithm generalized regression neural network (GRNN) was selected and its performance was higher than the RMBF method [25] [26], Hargreaves and Blaney-Criddle.

In another study [12], the methods of ET estimation can be classified in two categories:

(i) semi- empirical methods, which utilize empirical relationship and a minimum of meteorological data.

(ii) analytical methods, which involve the establishment of the physical process at the scale of interest.

Grid computing technique is the act of sharing tasks over multiple computers. These tasks can't be approached without an enormous amount of computing power. They can range from data storage to complex calculations and can be spread over large geographical distances. Through Grid computing, the resources of many computers can be cooperatively managed as collaboration toward a common objective (Fig.1).

A Grid computing system generally comprises two types of grid systems, namely, Computational Grids and Data Grids. The key role of the Computational Grids is to provide solutions of the intricate scientific or engineering problems that use complex and computational intensive problem-solving algorithms, for example, medical diagnoses or satellite image processing.

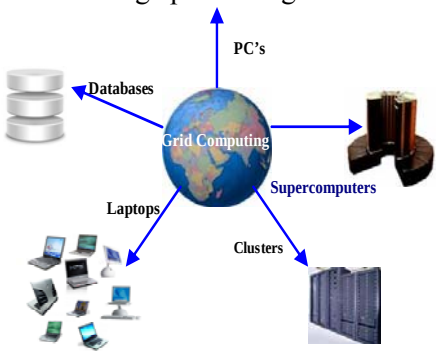

Fig.1. Grid Computing

These applications use services of a Data Grid in order to access the distributed data sets in a distributed networked environment. So, the key role of a Data Grid is to provide the backbone on which a Computational Grid performs its operation

Due to satellite images large size – up to 1 GB, Grid based architectures might be suitable platforms for their digital processing and analysis, because they offer the required computational power to process satellite data in real time [13].

The emergency of the Grid computation method offers two major advantages:

(i) strong data-processing capability and

(ii) the ability to use distributed computing resources to process the spatial data provided by a satellite image.

Sumarizing, the objective of this paper is to develop a Grid computing application (a Computational Grid), which estimates the evapotranspiration at regional scale using the remote sensing data and a minimal amount of ground data.

This paper is organized in 4 sections. The first section is Introduction and the second presents the Problem Formulation. In section 3, we describe the application that uses the Computational Grid and the experimental results. Conclusion and further work are approached in section 4.

2 Problem Formulation

The model used to ET estimation is based on the Triangle method. This method use the Priestly-Taylor equation modified by Jiang and Islam [10], where the α coefficient is a function of land surface temperature (LST) and Normalized Difference Vegetation Index (NDVI) [16].

The original formula of Priestly-Taylor equation is:

$$\lambda E = \alpha \cdot \left[(R_n - G) \cdot \frac{\Delta}{\Delta + \gamma} \right], \quad (1)$$

where:

λE is the latent heat flux,

α is an empirical parameter,

R_n is the net radiation (including long wave and short wave),

G is the soil heat flux,

Δ is the slope of saturated vapor pressure,

γ is the psychometric constant.

The "beauty" of this equation is that all terms can be calculated using remotely sensed data.

According with Jiang and Islam [10] the parameter α is obtained by two-step linear interpolation scheme:

- In the first step, the upper and lower bounds of α for each specific NDVI class is obtained; NDVI classification is determined from the land use map.

In our study, there are three main land uses: water, urban, barren land and vegetation. We consider a NDVI class for each NDVI value of the main land uses.

The second step is to range the parameter α within each NDVI class between the lowest temperature pixel and the highest temperature pixel. For this interpolation the relationship between LST and NDVI is used. Thus, the equation of the parameter α is:

$$\alpha = \left(\frac{\Delta + \gamma}{\Delta} \right) \cdot \left(\frac{NDVI_i^{\max} - NDVI_i^{\min}}{NDVI_i^{\max}} \right) \cdot \left(\frac{LST_i^{\max} - LST}{LST_i^{\max} - LST_i^{\min}} \right) + \left(\frac{\Delta + \gamma}{\Delta} \right) \cdot \left(\frac{NDVI_i^{\min}}{NDVI_i^{\max}} \right) \quad (2)$$

where:

- LST is value for current pixel,

- $LST_i^{\max}$, $LST_i^{\min}$ are the maximum and minimum values of surface temperature

- $NDVI_i^{\max}$, $NDVI_i^{\min}$ are NDVI, respectively, within the NDVI class which has the current pixel.

Finally, the daily value of ET is:

$$\lambda E_{daily} = \left[\left(\frac{NDVI_i^{\max} - NDVI_i^{\min}}{NDVI_i^{\max}} \right) \cdot \left(\frac{LST_i^{\max} - LST}{LST_i^{\max} - LST_i^{\min}} \right) + \left(\frac{NDVI_i^{\min}}{NDVI_i^{\max}} \right) \right] \cdot \frac{2DL \cdot (R_i - G_i)}{\pi \cdot \sin(\pi \cdot t / DL)} \quad (3)$$

where:

- DL is total day length, hours,

- t is time beginning at sunrise.

To obtain the 24 hours totals, the daily ET values are multiplied by 1.1 for all days.

To compute the LST we implemented the Jimenez - Munoz and Sobrino's algorithm [21] which needs a single ground data (the total atmospheric water vapor content – w).

In order to calculate the LST, we firstly compute the NDVI, by:

$$NDVI = \frac{band4 - band3}{band4 + band3} \quad (4)$$

and the Land Surface Emissivity (LSE), based on NDVI values [20]:

$$LSE = 1.0094 + 0.047 * \ln(NDVI) \quad (5)$$

When the NDVI value is out of the range (0.157–0.727), the corresponding input LSE constant values are used [20].

Now, we can calculate LST:

$$LST = \gamma [LSE^{-1} \cdot (\psi_1 L_{sensor} + \psi_2) + \psi_3] + \delta, \quad (6)$$

with

$$\gamma = \left\{ \frac{c^2 L_{sensor}}{T_{sensor}^2} \left[\frac{\lambda^4}{c_1} L_{sensor} + \lambda^{-1} \right] \right\}^{-1} \quad (7)$$

and

$$\delta = -\gamma L_{sensor} + T_{sensor}, \quad (8)$$

where:

$$L_{sensor} = gain * DN + bias$$

is the spectral radiance,

DN is the digital number of a pixel,

$$T_{sensor} = \frac{K_2}{\ln(K_1 / L_{sensor} + 1)}$$

is the brightness temperature

λ - the effective wavelength,

$c_1 = 1.19104 * 10^8 W \mu m^4 m^{-2} sr^{-1}$,

$c^2 = 14387.7 \mu m K$,

$\psi_i, i = \overline{1,3}$ are atmospheric parameters, obtained as functions of the total atmospheric water vapor content (w) .

The net radiation R_n was computed by [18]:

$$R_n = R_s (1 - a) + \varepsilon_a \sigma T_{air}^4 - LSE \sigma LST^4 \quad (9)$$

where:

- R_n is the net radiation at the ground surface in W/m^2,
- R_s is the total incoming radiation at the ground surface in W/m^2,
- a is the surface broadband albedo,
- ε_a is the atmospheric emissivity,

$$\varepsilon_a = 1.08 * (-\ln \tau)^{0.265} \text{ (dimensionless)},$$

- τ - the atmospheric transmissivity,
- σ - the Stefan - Boltzmann constant,
- T_{air} is the atmospheric temperature near ground surface in K.

According to [14], the surface broadband albedo a can be retrieved based on the spectral albedo for Landsat TM/ETM+ data, by the formula:

$$a = 0.356\rho_1 + 0.130\rho_3 + 0.373\rho_4 + 0.085\rho_5 + \\ + 0.072\rho_7 - 0.0018 \quad (10)$$

where ρ_i is the at-surface reflectance in band i for Landsat data.

The soil heat flux G is the rate of heat storage in a soil, as a result of temperature gradient between soil surface and the underlying topmost soil layers. To calculate it we used an empirical relationship [2] which attempts to estimate G as a function of NDVI, surface temperature and albedo, by:

$$G = R_n \frac{LST - 273}{a}[0.0032 \cdot (1.1a) + 0.0062 \\ \cdot (1.1a)^2](1 - 0.978 \cdot NDVI^4) \quad (11)$$

For the calculation of evapotranspiration, the slope of the relationship between saturation vapors pressure and temperature, Δ, is also required. The slope of the curve at a given temperature is given by:

$$\Delta = \frac{4098 \cdot \left[0.6108 \exp\left(\frac{17.27 T_{air}}{T_{air} + 237.3}\right)\right]}{(T_{air} + 237.3)^2}, \quad (12)$$

where T_{air} is the air temperature in ^{0}C.

3 Study area and data

3.1. About Dobrogea

Dobrogea region has been chosen for this study due to its importance in the Romanian economy. Dobrogea together with Romanian plain and South of Moldova are among the driest areas, where the crops cannot grow without irrigation systems. It is absolutely necessary to know ET as management method of the water sources for irrigation, for the design and exploitation of the irrigation systems.

Dobrogea is a region situated in the South – East of Romania, between the Black Sea and the lower Danube River (Fig.2).

Dobrogea (without the Danube Delta) is a plateau with hilly aspect. Generally, it has a temperate - continental climate. The air average temperature is slightly over 11^{0}C towards the littoral area and the Danube floodplain, and no more than 10 - 11^{0}C in the North and center [15].

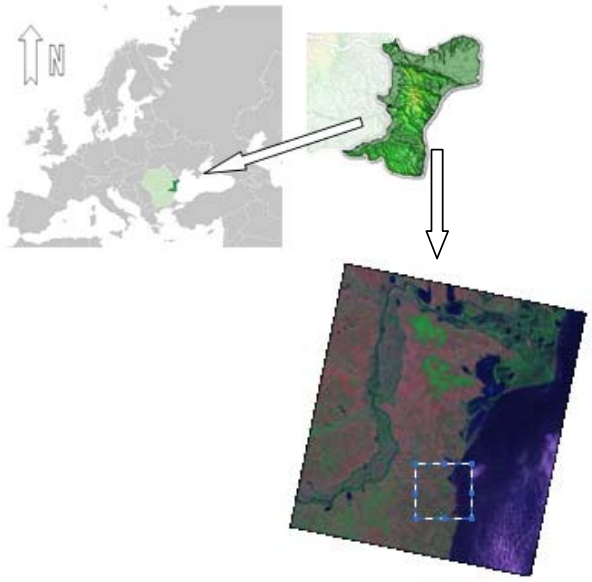

Fig. 2. Dobrogea area and Landsat ETM+ "false color" image; bands combination: 742

3.2. Satellite Data

In this study, we used one subset of Landsat ETM+ image dated 7th June 2000 that covers the Dobrogea area corresponding to Constanta weather station. The image is in geo-tiff format and was downloaded from Landsat Imagery [11]. A radiometric calibration (atmospheric corrections) was the pre-processing step that was taken. The bands ETM+ 3 and 4 were analyzed with respect to the NDVI values, the band ETM+ 6 was used to compute the LST values, and the other bands (ETM+ 1, 2, 5 and 7) were processed to estimate the albedo values.

3.3. Meteorological Data

In addition to satellite data, this study needed two ground meteorological data:

- the total atmospheric water vapor content, w, used in LST estimation algorithm,
- the air temperature - T_{air}.

These parameters were obtained from the weather station of Constanta, located on the study area. The weather conditions prevailing on 7th June

2000 are shown in table 3.

4 Problem Solution

4.1 Satellite Data Pre-processing

Satellite data pre-processing comprise of radiometric calibrations (atmospheric corrections) for ETM+ bands 3 and 4. These bands are used to retrieve NDVI (Normalized Difference Vegetation Index) values on which the LST (land Surface Temperature) estimation algorithm is based on. It is possible to obtain NDVI values from at-sensor or TOA (Top of Atmospheric) reflectivity, called as $NDVI_{TOA}$, but it is more accurate to atmospherically correct the TOA values in order to obtain at-surface reflectivity and, in this way, estimate NDVI values more representative of the natural surfaces, called as $NDVI_{surf}$.

In this study we applied an atmospheric correction based on image data, developed by [4]. Its main advantage is that the data necessary to carry out the atmospheric correction are obtained from the image itself.

The at-surface reflectivity is calculated with the following equation:

$$\rho_{surf} = \frac{\pi(L_{sensor} - L_p)d^2}{E_0 \cos\theta_z T_z}, \quad (13)$$

where:

- L_{sensor} is at-sensor radiance,
- T_z is the atmospheric transmissivity between the sun and the surface:

$$T_z \approx \cos\theta_z \text{ [5]},$$

- θ_z is the zenithal solar angle,
- E_0 is the spectral solar irradiance on the top of the atmosphere [3],
- d is the Earth–Sun distance [3],
- L_p is the radiance resulted from the interaction between the electromagnetic radiance and the atmospheric components (molecules and aerosols) that can be obtained according to:

$$L_p = L_{\min} - L_{1\%}, \quad (14)$$

where:

- $L_{\min}$ is the radiance that corresponds to a digital count value for which the sum of all the pixels with digital counts lower or equal to this value is equal to the 0.01% of all the pixels from the image considered.

$L_{\min}$ was calculated through DOS (Dark Object Subtraction) technique [5].

- $L_{1\%}$ is given by:

$$L_{1\%} = \frac{0.01\cos\theta_z T_z E_0}{\pi d^2} \quad (15)$$

4.2. Approach

Our application meets the requirements of a virtual organization (VO) member which has access to a local database of large satellite images and wants to apply several satellite image processing operations in order to estimate the daily evapotranspiration. The operations to be performed are implemented in special client's codes and are to be run on the Computational Grid.

Due to the large size of a satellite image, the full image transfer should be avoided. Therefore, a satellite image will be split into a number of sub-images equal with the number of workstations of the Grid Cluster. The image processing algorithms will also be split into independent tasks that can be performed in parallel and that are requiring similar computing effort.

The design applied is called the Split and Aggregate design which allows to parallelize the process of task execution gaining performance and scalability.

Fig. 3 (http://www.gridgain.com/) shows the logical steps on a Computational Grid: a Grid task splits into Grid jobs that are executed on Grid nodes, the results of the jobs are then aggregated into one, namely the Grid task result.

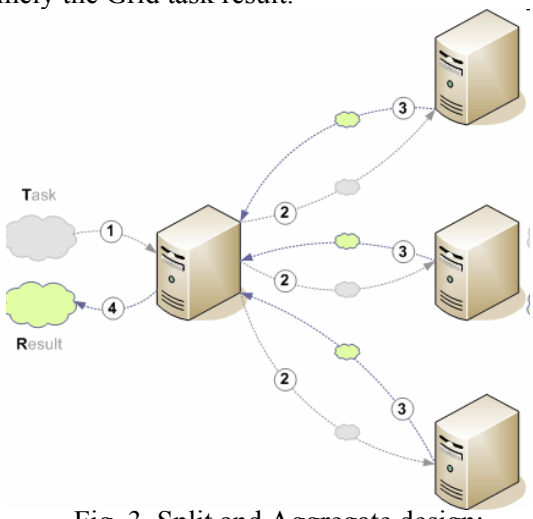

Fig. 3. Split and Aggregate design:
1. Grid task execution request; 2. Grid task splits into Grid jobs; 3. Result of job execution; 4. Aggregation of job results into Grid task result

The following components are necessary:

- at the user's node: the satellite bands, the client's codes and some minimal facilities to access Grid infrastructure,
- at remote computing nodes: the Grid middleware which allows the execution of client's codes.

The client's code consists of three components (Fig.4).

- the Splitter that takes a satellite image and split it into a number of sub-images;
- the Image ET Estimator, that receives a sub-image, applies the processing algorithms and produces the output files (LST image, ET image and 3 text files of NDVI, LST and ET float values);
- the Composer that merges the resulting sub-images.

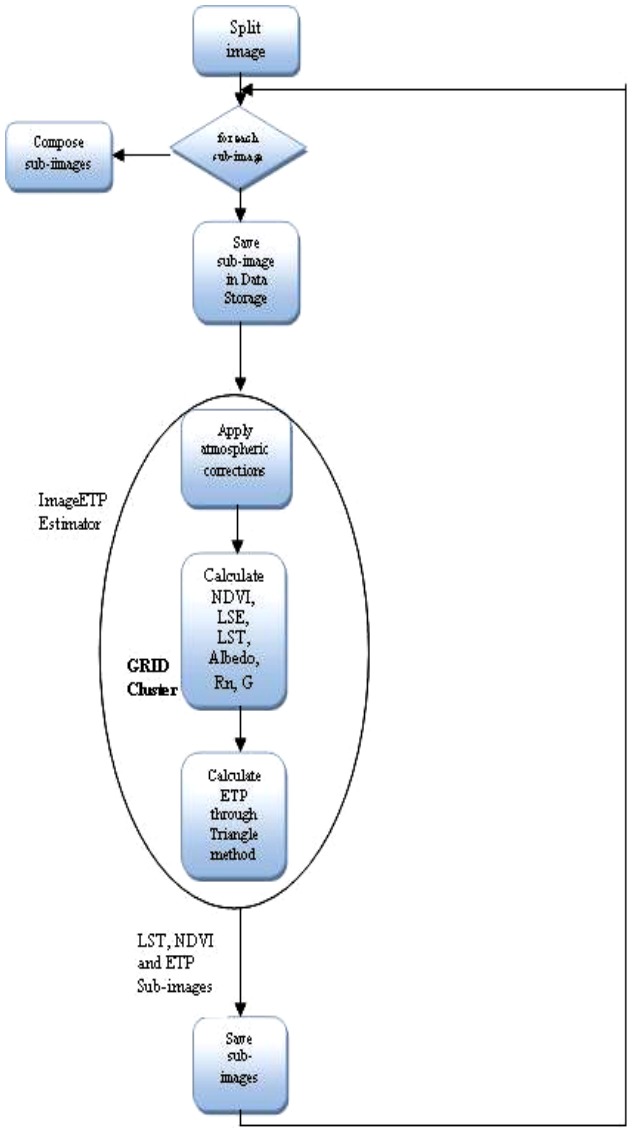

Fig. 4. The logical processing steps of each sub-image

The Splitter and the Composer programs run only at the user's site where the large satellite images are residing. The Image ET Estimator and the sub-images are submitted for processing on the Computational Grid.

The user uploads the image files and submits the jobs to the Grid.

After the successful finish of the jobs, the user can download the resulting images.

The service works as follows (Fig. 5):

- the user uploads the image files using Grid FTP and submits the job to the Grid;
- the image file(s) are transferred to code site;
- the Splitter code is called and the smaller pieces of image(s) are produced as well as the files needed by PBS to launch the Image ET Estimator operation on each sub-image;
- The Job Manager of Globus Toolkit 4 takes over the files and interpret them and finally PBS sends the jobs on the cluster of workstations;
- After the job executions the output files are stored on the code site.

The user can access the output files through the user interface.

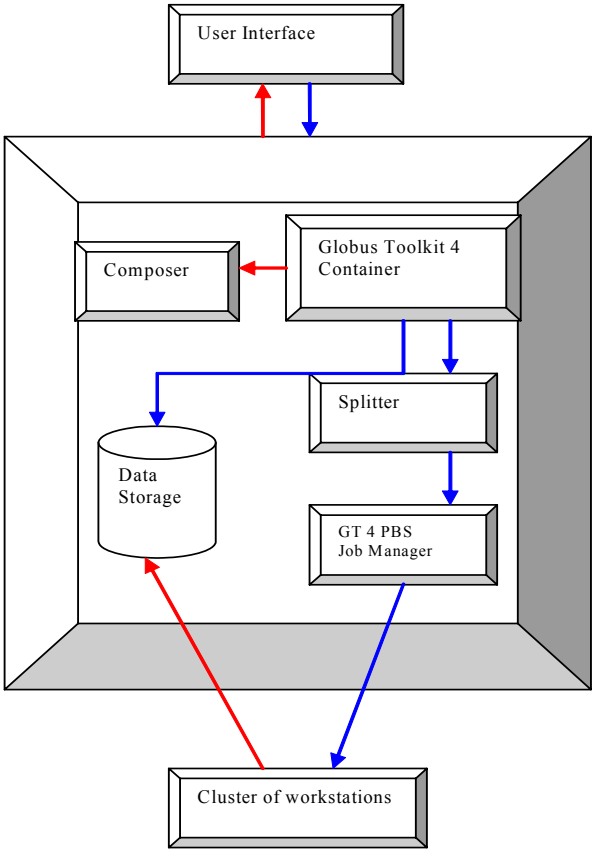

Fig.5. The components of the service and their interactions

The client's code was written in Java and tested using Python scripts (Figs. 6 and 7) on the Computational Grid provided by Globus Toolkit 4.

```
submitCommandTemplate = "${GLOBUS_LOCATION}/bin/globusrun-ws -submit
        -s -batch -o subimage%02d.epr -F %s -Ft %s -f %s"

# choose randomly the PBS or SGE factory
factoryType =random.choice(['PBS','SGE'])
factory = factoryCatalog[factoryType]

jobDescriptionFilePath = createGridJobDescriptionFile(subimageNumber)

submitCommand = submitCommandTemplate % (subimageNumber,factory,
       factoryType,jobDescriptionFilePath)
print "Preparing to submit job to grid..."
print "Submit command: %s" % submitCommand
try:
      job = popen2.Popen3(submitCommand, capturestderr = True)
      jobOut = []
      jobErr = []
      ret = job.poll()
      while ret == -1:
            jobOut.extend(job.fromchild.readlines())
            jobErr.extend(job.childerr.readlines())
            time.sleep(1)
            ret =  job.poll()
except Exception, e:
            msg = "Error while submitting GRAM WS job: %s" % e
            raise RuntimeError, msg
```

Fig.6. Python script for code testing

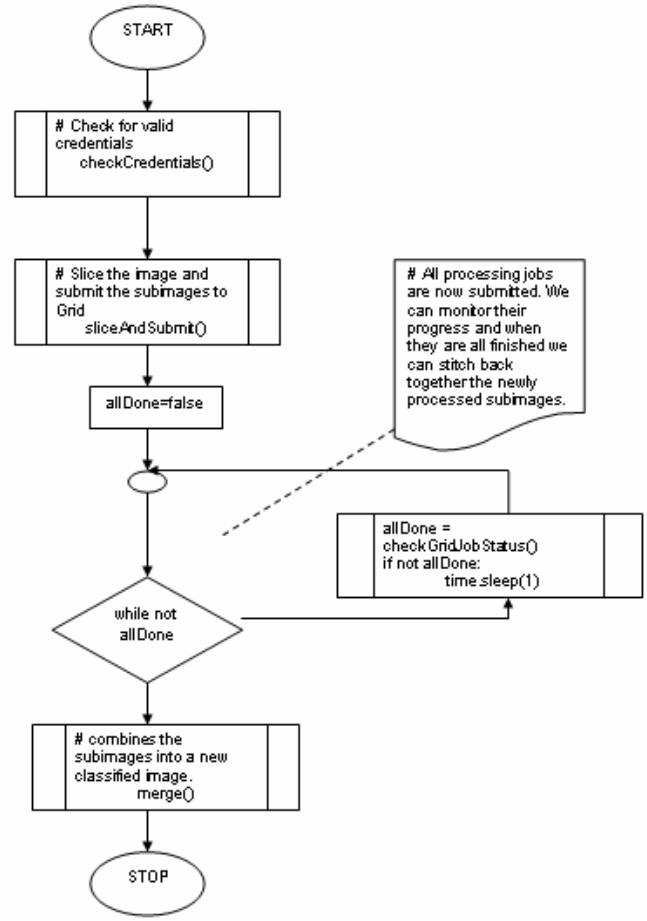

Fig. 7 Python script flowchart

A Web - based client interface (Fig.8), for a service that launches the codes has also been built using JSP, Tomcat/5.5 and MySQL.

The testing environment contains 2 PC nodes (Intel P4, 2.4 GHz, 1GB DDRAM) connected at 100 Mbps and allows processing images of size up to 10 MB.

The tests performed by us proved that the presented application is efficient in terms of computation time and easy to use (Table 1). The application output data consist of the files described in Table 2.

Table 1. Response time for the sub-images processing

No. of nodes	Response time (s)	File Size
1	8.641	1500 x 1500
2	2.831	750 x 750

Table 2. The output data

File	Description
.txt	Text file with LST values (^{0}C)
.txt	Text file with NDVI values
.txt	Text file with daily ET values
.txt	Text file with statistical data for each NDVI class (min, max, mean, stdev. of NDVI, LST and ET values)
.tiff	LST Map
.tiff	ET Map

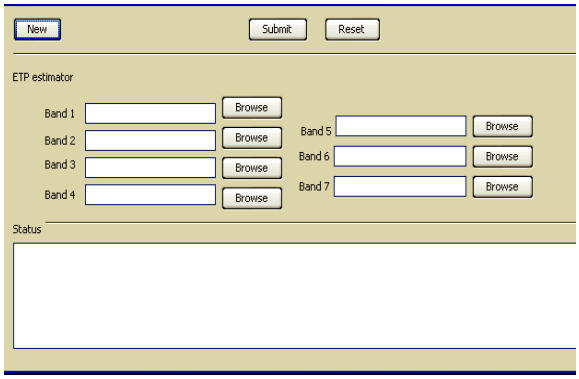

Fig.8. The user's interface

The area used in this study contains diverse land cover types, including vegetative area (dense or sparse), high and medium density built up spaces, and water bodies (Fig. 9).

The LST Map (Fig.10) shows that the LST values for the study area vary between 22^{0}C la 48^{0}C, which is consistent with the ground meteorological data measured by Constanta station (measurements are taken every 6 hours) (Table 3 and Fig.11). The highest LST values are obtained for the building area (40^{0}C - 48^{0}C). For the area covered by vegetation, the LST varies between 31^{0}C and 37^{0}C, the higher values being obtained for the sparse

vegetation spots. The lowest LST values were observed for water bodies.

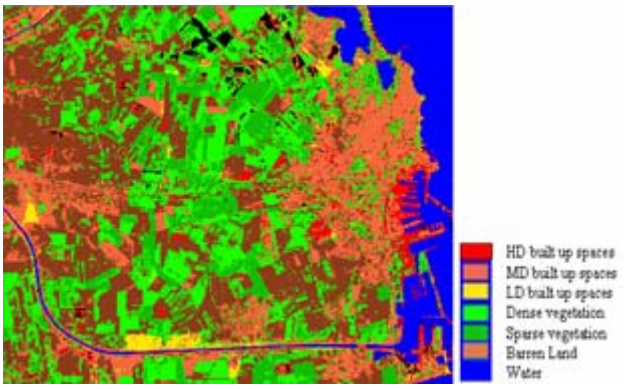

Fig.9. Land cover classification images, 2000

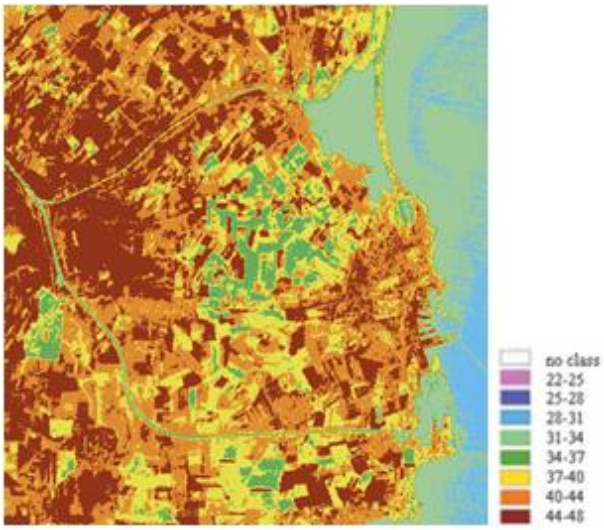

Fig.10. LST Image - Dobrogea region, 2000

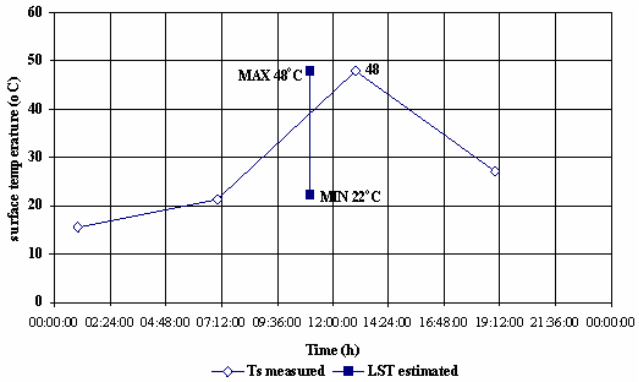

Fig.11. LST values measured and estimated

The error between the actual mean ground surface temperature at the time when satellite passed and the remote sensed mean land surface temperature (0.73^0C) is considered to be acceptable.

Table 3. Comparison between actual mean LST and remote sensed mean LST

Date:	June 7, 2000
Satellite Overpass Time	
GMT	8.32
Local Time	11.32
Weather Station Data	
Air Temp (^{0}C)	23.3
Humidity (%)	82
w (g/cm^2)	2.3
Mean LST (^{0}C)	
At 7 am:	21.2
At 13 am:	48
At 11.30 am:	42.31
Remote sensed LST	
Mean LST (^{0}C)	41.58

The spatial variation of evapotranspiration is shown in Fig. 12. Evapotranspiration ranges between 0.33 and 5.24mm/day. According to Constanta weather station, the multi-annual average of the evapotranspiration in June for Constanta area is between 4.5 and 5.6 mm/day, so the estimation error is eligible.

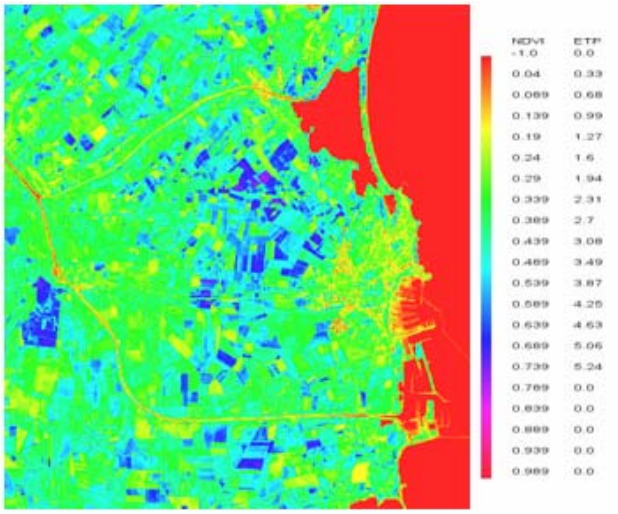

Fig. 12 ETP Image - Dobrogea region, 2000

5 Conclusion

In this paper we present a Computational Grid to estimate the daily ET values in Dobrogea region using remote sensing imagery. The application is meant to be used by those who want to do such studies but don't have the computational resources they need. We implemented an ET estimation algorithm, the Triangle method, which is based on the modified Priestly-Taylor equation and whose inputs are mainly satellite data. The proposed

approach is applied to Constanta area to estimate ET in 7th June 2010. The results are promising and show that the method utilized can derive reasonable estimates for surface temperature (LST) and evapotranspiration (ET). We consider that the application will be greatly useful and convenient for those who use satellite remote sensing to study the geographical distribution of evapotranspiration, and consequently water demand in large cultivated areas for irrigation purposes and sustainable water resources management, and have typical workstations, with no special computing and storing resources for computationally intensive satellite image processing, and no license for a commercial image processing tool.

Acknowledgements. This article was supported by CNCSIS – UEFISCSU under Grant PN II IDEI 262/2007.

References:

[1] Allen, G. R., Pereira, L. S., Raes, D and Smith, M. *Crop Evapotranspiration-Guidelines for computing crop water requirements FAO Irrigation and Drainage Paper 5,* FAO, Rome, Italy, 1998

[2] Bastiaanssen, W.G.M., Pelgrum, H., Wang, J., Ma, J., Moreno, J., Roerink, G.J., Van Der Wal, T., *The Surface Energy Balance Algorithm for Land (SEBAL): Part 2 validation.* J. Hydrol. 228, 213-229, 1998

[3] Chander, G., Markham, B L., Helder, D.L,. *Summary of current radiometric calibration coefficients for Landsat MSS, TM, ETM+, and EO-1 ALI sensors*, Remote Sensing of Environment 113, 2009, pp. 893–903

[4] Chavez P.S., *An improved dark-object subtraction technique for atmospheric scattering correction of multispectral data*, Remote Sensing of Environment, 24, 1988, pp. 459-479

[5] Chavez, S., *Image-based atmospheric correction—revisited and Improved*, Photogrammetric Engineering and Remote Sensing, 62(9), 1996, pp. 1025– 1036,

[6] Courault, D., Seguin, B., Olioso, A., *Review to estimate evapotranspiration from remote sensing data: some examples from the simplified relationship to the use of mesoscale atmospheric models,* an ICID workshop on remote sensing of ET for large regions, Montpellier, France, 2003, pp. 1-17

[7] Harmsen E. W., Mecikalski J., Cardona-Soto M.J., Rojas Gonzalez A., Vasquez R., *Estimating Daily Evapotranspiration in Puerto Rico using Satellite Remote Sensing*, WSEAS Transactions on Environment and Development, Vol. 6(5), 2009, pg. 456-465

[8] Harmsen E. W., Ramirez Builes V. H., Dukes M. D., Jia X., Gonzalez J. E., Perez Alegia L. R., *A Ground-Based Method for Calibrating Remotely Sensed Surface Temperature for use in Estimating Evapotranspiration*, WSEAS Transactions on Environment and Development, Volume 5, 2009, pp. 13-23

[9] Jacob, B., Brown, M., Fukui, K., Trivedi, N., *Introduction to Grid Computing,* SG24-6778-00 2005, http://ibm.com/redbooks,

[10] Jiang, L. and Islam, S. *Estimation of surface evaporation map over southern Great Plains using remote sensing data*, Water Resour. Res., Vol. 37(2), 2001, pp.329-340,

[11] Landsat Imagery, http://www.landsat.org/ortho/index.php

[12] Li Zhao Liang, et al., *A Review of Current Methodologies for Regional Sensed Data*, Sensor Data, 9, 2009, pp. 3801-3853

[13] Li Sheng-yang, Zhu Chong-guang, GE Ping-ju, *Remote Sensing Image Deblurring, Based on Grid Computation,* J. China Univ. of Mining & Tech. (English Edition), Vol. 16(4), 2006, pp. 409-412.

[14] Liang, S., *Narrowband to broadband conversions of land surface albedo I algorithmes,* Remote Sensing of Environment, 76, , 2000, pp. 213-238

[15] Maftei, C., Bărbulescu, A., *Statistical analysis of climate evolution in Dobrudja region*, Lecture Notes in Engineering and Computer sciences, WCE, vol.II, 2008, pp. 1082 -1087

[16] Nourbaeva, G., Kazama, S., Sawamato, M., *Assesment of Daily Evapotranspiration Using Remote Sensing Data*, Environmental Informatics Archives, Vol 1, 2003, pp. 421-427

[17] Petcu, D. *Arhitecturi si tehnologii Grid*, Editura Eubeea, 2006

[18] Sheng, P., Mao, J., Li, J., et al.. *Atmospheric Physics*, Peking University Press, Beijing, 2003, pp. 107-115

[19] Singh, V. P. and Xu, C. Y., *Evaluation and Generalization of 13 Mass-transfer Equations for determining free water evaporation*, Hydrological Processes, Vol. 11, 1997, pp. 311-323.

[20] Sobrino J., Raissouni N., Li Z., *A comparative study of land surface emissivity retrieval from NOAA data*, Remote Sensing of Environment, 75, , 2001, pp. 256-266

[21] Sobrino J., Jimenez-Munoz J.C., Paolini L., *Land surface temperature retrieval from LANDSAT TM 5*, Remote Sensing of Environment 90, 2004, pp. 434–440

[22]Remote Sensing Guide, http://cbc.rs-gis.amnh.org/

[23] Traore S., Wang Y.M., Kerh T., *Modeling reference evapotranspiration by generalized regression neural network in semiarid zone of Africa*, WSEAS Transactions on Information Science and Applications, Vol. 5, 2008, pp. 991-1000,

[24] Wallace, J.S. *Calculating evaporation: resistance to factors,* Agricultural and Forest Meteorology Vol. 73(3-4), 1995, pp. 353-366

[25] Wang Y.M., Traore S., Kerh T., *Assessment of evapotranspiration based on data information models at production sites in Burkina Faso*, WSEAS Transactions on Computers, Vol.6, No.6, 2007, pp. 880-887

[26] Wang Y.M., Traore S., Kerh T., *Determination of a Reference Model forEstimating Evapotranspiration in Burkina Faso*, Proceedings of the 6th WSEAS Int. Conf. on Artificial Intelligence, Knowledge Engineering and Data Bases, Corfu Island, Greece, February 16-19, 2007

[27] Zhigang Sun, Qinxue Wang, Bunkei Matsushita, Takehiko Fukushima, Zhu Ouyang,Masataka Watanabe *Development of a Simple Remote Sensing EvapoTranspiration model(Sim-ReSET): Algorithm and model test* Journal of Hydrology, 376, 2009, pp. 476–485